Journal of Engineering Physics and Thermophysics, Vol. 81, No. 2, 2008

HYDRO- AND GAS DYNAMICS IN TECHNOLOGICAL PROCESSES

NUMERICAL SIMULATION OF FREE CONVECTION OF A HEAT-RELEASING FLUID IN AN AXISYMMETRIC CLOSED VOLUME

D. G. Grigoruk, P. S. Kondratenko, and D. V. Nikol'skii

UDC 536.24

A simplified computing method has been developed and on its basis the problem on laminar free convection of a heat-releasing fluid in a cylindrical and a hemispherical volumes with an isothermal lateral (in the case of a hemisphere, lower) and adiabatic upper bounds has been solved. On the basis of the results obtained the influence of the temperature stratification in the volume and geometry on the heat transfer characteristics has been investigated. It has been established that neglecting the temperature stratification leads to a considerable overestimation of the density of heat flow to the boundary in the lower part of the volume.

Introduction. The problem of providing safety of nuclear power engineering objects has revealed the necessity of investigating the class of free convective flows caused by internal heat sources rather than by external conditions. In a bad accident at an NPP for medium- and low-power water-moderated water-cooled reactors the problem of preserving integrity of the vessel arises. In the case of loss of the coolant, the reactor core under the action of heat loads begins to break and fuse. To prevent breakage of the vessel and release of radioactive materials, its outer boundary is cooled with water. The efficiency of such cooling is determined by the mechanism of boiling on the volume surface. This mechanism in turn depends on the local distribution of the heat flux to the boundary due to the free convection of the heat-releasing melt. When the heat flux density reaches a critical value, then the so-called boiling crisis occurs. It corresponds to the nucleate-film boiling transition. In this process, the cooling efficiency markedly decreases, leading to melting of the reactor vessel. The character of free convection is determined by the afterheat power and thermophysical properties of the melt, as well as by the shape of the volume surface.

The solution of the complete system of equations describing the convective flow of a fluid with internal heat sources requires much time and considerable computational expenditures. At the same time, to determine the consequences of a bad accident at an NPP with reactor core melting, it is necessary to estimate the distribution of the heat transfer of the melt to the reactor vessel in the shortest possible time. To this end, various simplified models are used in the reactor codes [1, 2]. In the present work, we have constructed a physical model and developed an algorithm for solving the problem on free convective heat transfer of a single energy-releasing fluid in a closed volume. The medium was assumed homogeneous, incompressible, isotropic with constant thermophysical properties, and with a positive thermal expansion coefficient, and the flow conditions were considered to be laminar. The problem on the convection in a cylindrical and hemispherical volumes in the range of modified Rayleigh numbers $10^6 \le \mathrm{Ra_i} \le 10^{12}$ has been solved.

Formulation of the Problem. Consider a stationary free convection of a heat-releasing fluid in an axisymmetric volume with an isothermal lateral (lower in the case of a hemisphere) boundary. As experiments, theoretical analysis, and numerical calculations show [3–7], the volume can be broken down into three flow regions (see Fig. 1).

Institute for Problems of Safe Development of Nuclear Power Engineering, RAS, 52 Bol'shaya Tul'skaya Str., Moscow, 115191; email: grig@ibrae.ac.ru. Translated from Inzhenerno-Fizicheskii Zhurnal, Vol. 81, No. 2, pp. 280–289, March–April, 2008. Original article submitted March 13, 2006.

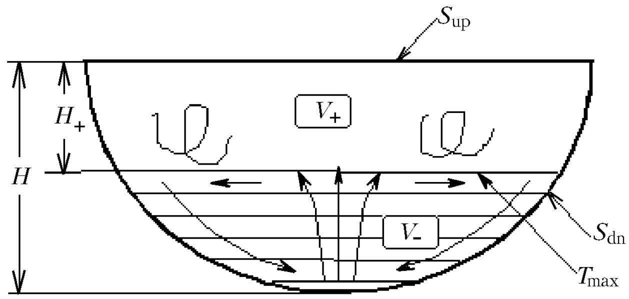

Fig. 1. General structure of the flow.

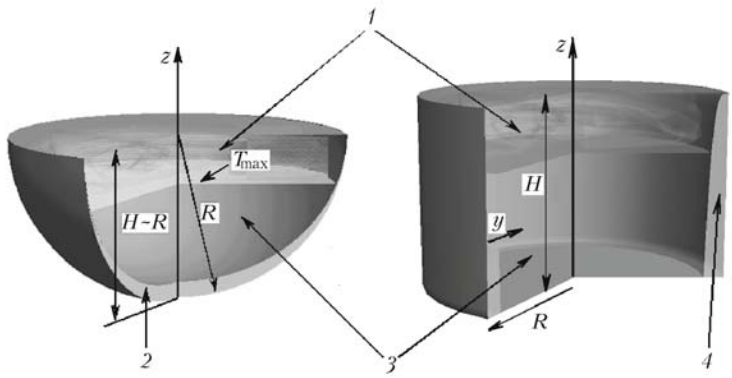

Fig. 2. Geometry of the problem: 1) Rayleigh–Benard layer (the case of the cooled upper boundary); 2) boundary layer on the bottom; 3) region of stable temperature stratification; 4) boundary layer on the side wall.

1. Structurally inhomogeneous flow near the upper horizontal boundary. The horizontal plane passing through the maximum point of the time-average value of the fluid temperature divides the volume into two parts. In the case of cooling the fluid surface S_{up} in the region V_+ of height H_+, by virtue of the inverse temperature distribution, a situation close to the conditions for Rayleigh–Benard convection is formed. The given flow is characterized by a decrease in the temperature with approach to he plane upper boundary and the thus arising positive density gradient in the direction opposite to the direction of the gravity force.

2. Region of boundary layers. Heat transfer through the lateral boundary occurs through a thin boundary layer (BL), in which the fluid moves by gravity to the bottom, accelerating due to the inflow of the fluid from the main volume (region outside the boundary layers). However, with approach to the bottom there occurs a deceleration of the BL followed by the return of the fluid into the main volume. Near the bottom the fluid, having changed its direction, moves to the volume axis where it finally decelerates. In the case of hemispherical geometry, where the lower and lateral surfaces represent a whole, the BL is convergent, due to which the flow changes its direction continuously.

3. Region of stable stratification. A slow upward flow outside the boundary layer in the lower part of the volume V_- occurs under the conditions of stable temperature stratification.

Due to the existence of three clearly defined flow regions the problem on the distribution of the heat flux to the boundary of a closed volume can be simplified. We restrict ourselves to the consideration of the case where the upper horizontal boundary of the volume is heat-insulated. Then because of the temperature stratification in the main volume, the temperature maximum T_{max} is attained at the upper boundary and the regime of Rayleigh–Benard convection is not realized. Thus, let us assume that the whole of the volume occupied by the fluid consists of thin boundary layers (with thickness $\delta << H$, R) and a temperature stratification region (see Fig. 2).

To describe the steady fluid flow in the boundary layer on the vertical boundary, let us make use of the Prandtl approach [8]. Since the BL thickness δ is much smaller than the characteristic cross-section of the volume R, the energy release on the right-hand side of the equation can be neglected [9], and the system takes on the following form:

cylinder

$$\frac{\partial u}{\partial z} + \frac{\partial v}{\partial y} = 0 \, , \tag{1}$$

$$u \frac{\partial u}{\partial z} + v \frac{\partial u}{\partial y} - \nu \frac{\partial^2 u}{\partial y^2} = g\beta \, (T - T_\mathrm{b} \, (z)) \, , \tag{2}$$

$$u \frac{\partial T}{\partial z} + v \frac{\partial T}{\partial y} = \chi \frac{\partial^2 T}{\partial y^2} \, ; \tag{3}$$

hemisphere

$$\frac{1}{R \sin (\theta)} \frac{\partial}{\partial \theta} (\sin (\theta) \, u) + \frac{\partial v}{\partial y} = 0 \, , \tag{4}$$

$$u \frac{\partial u}{\partial \theta} + v \frac{\partial u}{\partial y} - \nu \frac{\partial^2 u}{\partial y^2} = g\beta \, (T - T_\mathrm{b} \, (z)) \sin (\theta) \, , \tag{5}$$

$$u \frac{\partial T}{\partial \theta} + v \frac{\partial T}{\partial y} = \chi \frac{\partial^2 T}{\partial y^2} \, . \tag{6}$$

The boundary conditions for system (1)–(6) are:
cylinder

$$y = 0 : \;\; u, v, T - T_0 = 0 \, , \;\; y >> \delta : \;\; u \to U \, (z) \, , \;\; T \, (z, y) - T_\mathrm{b} \, (z) \to 0 \, ; \tag{7}$$

hemisphere

$$y = 0 : \;\; u, v, T - T_0 = 0 \, , \;\; y >> \delta : \;\; u \to U \, (z) \, , \;\; T \, (y, \theta) - T_\mathrm{b} \, (z) \to 0 \, ; \;\; z = R \, (1 - \cos (\theta)) \, . \tag{8}$$

The temperature of the isothermal part of the boundary T_0 is taken as zero. Due to the stable temperature stratification (the temperature is independent of the horizontal coordinates and $dT_\mathrm{b}/dz > 0$) the energy balance equation in the main volume is of the form [9]

$$U \, (z) \frac{dT_\mathrm{b} \, (z)}{dz} = \frac{Q}{\rho c_p} \, . \tag{9}$$

From the mass balance condition it follows that the mass flow through any section of the volume with a fluid is equal to zero. Hence we find the relation for the vertical velocity component relating it to the corresponding velocity component in the boundary layer:
cylinder

$$U(z) \cong -\frac{2}{R}\int_0^{\Delta} dy\, u(z, y)\,; \tag{10}$$

hemisphere

$$U(z) \cong -\frac{2}{R\sin(\theta)}\int_0^{\Delta} dy\, u(\theta, y)\,, \quad z = R(1-\cos(\theta))\,. \tag{11}$$

Here the value of the upper limit in the integral is chosen in accordance with the inequality $\delta << \Delta << R$.

Since the temperature in the main volume is an increasing function of height, in the relative proximity to the bottom its value is low compared to the mean value throughout the volume. Moreover, as experiments and theoretical estimates show [9], the BL thickness on the volume bottom is much larger than on the lateral surface. For this reason we neglect the heat transfer into the bottom. As a result, at $z \to 0$, similarly to (10), (11), from the energy balance equation a relation relating the temperatures in the boundary layer and in the main volume follows:

cylinder

$$U(0)\, T_{\text{b}}(0) \cong -\frac{2}{R}\int_0^{\Delta} dy\, u(0, y)\, T(0, y)\,; \tag{12}$$

hemisphere

$$U(0)\, T_{\text{b}}(0) \cong -\frac{2}{R\sin(\theta_0)}\int_0^{\Delta} dy\, u(0, y)\, T(0, y)\,, \tag{13}$$

where θ_0 is chosen smaller or of order $\arccos\left(1-\frac{\Delta}{R}\right)$ on the assumption of a homogeneous heat flux distribution near the pole [9].

Numerical Model. In terms of the dimensionless variables $\tilde{z}$, $\tilde{y}$, $\tilde{u}$, ... determined by the equalities

$$\begin{gathered}\tilde{z} = z/H\,, \quad \tilde{y} = y/\Delta\,, \quad \tilde{u} = u/A_u\,, \quad \tilde{v} = v/\left(A_u\frac{\Delta}{H}\right), \\ \tilde{T} = (T - T_0)/A_T\,, \quad \tilde{T}_{\text{b}} = (T_{\text{b}} - T_0)/A_T\,, \quad \tilde{U} = A_u\frac{\Delta}{R}U\,,\end{gathered} \tag{14}$$

where $A_u = \frac{\nu H}{\Delta^2}\left(\frac{\Delta}{R}\right)^{-1}$, $A_T = \frac{A_u^2}{g\beta H}$, the system of equations (1)–(7) describing the energy-releasing fluid flow in a closed volume takes the form

boundary layer

$$\frac{\partial\tilde{u}}{\partial\tilde{z}} + \frac{\partial\tilde{v}}{\partial\tilde{y}} = 0\,, \tag{15}$$

$$\tilde{u}\frac{\partial\tilde{u}}{\partial\tilde{z}} + \tilde{v}\frac{\partial\tilde{u}}{\partial\tilde{y}} - \frac{\Delta}{R}\frac{\partial^2\tilde{u}}{\partial\tilde{y}^2} = \tilde{T} - \tilde{T}_{\text{b}}\,, \tag{16}$$

$$\tilde{u}\frac{\partial\tilde{T}}{\partial\tilde{z}} + \tilde{v}\frac{\partial\tilde{T}}{\partial\tilde{y}} = \text{Pr}^{-1}\frac{\Delta}{R}\frac{\partial^2\tilde{T}}{\partial\tilde{y}^2}\,; \tag{17}$$

main volume (*including the boundary layers on the horizontal surfaces*)

$$\widetilde{U}\frac{d\widetilde{T}_{\mathrm{b}}}{d\widetilde{z}}-\mathrm{Pr}^{-1}\left(\frac{\Delta}{R}\right)^{2}\left(\frac{R}{H}\right)^{2}\frac{d^{2}\widetilde{T}_{\mathrm{b}}}{d\widetilde{z}^{2}}=\mathrm{Ra_i}\,\mathrm{Pr}^{-2}\left(\frac{\Delta}{R}\right)^{8}\left(\frac{R}{H}\right)^{6}; \tag{18}$$

mass balance

$$\widetilde{U}(\widetilde{z})=-2\int_{0}^{1}\widetilde{u}d\widetilde{y}; \tag{19}$$

energy balance (*the heat transfer into the bottom is neglected*)

$$\widetilde{U}(0)\,\widetilde{T}_{\mathrm{b}}(0)=-2\int_{0}^{1}\widetilde{u}(0,\widetilde{y})\,\widetilde{T}(0,\widetilde{y})\,d\widetilde{y}; \tag{20}$$

boundary conditions

$$\widetilde{u}\big|_{\widetilde{z}=1}=\widetilde{v}\big|_{\widetilde{z}=1}=\widetilde{u}\big|_{\widetilde{y}=0}=\widetilde{v}\big|_{\widetilde{y}=0}=\widetilde{T}\big|_{\widetilde{y}=0}=\widetilde{u}\big|_{\widetilde{y}=1}=0\,,\quad \widetilde{T}\big|_{\widetilde{y}=1}=\widetilde{T}_{\mathrm{b}}\,. \tag{21}$$

The calculations of Eqs. (15)–(20) was carried out on a uniform rectangular mesh. The cross-section of the region Δ was chosen so that the whole of the boundary layer was contained inside the calculated region ($\delta < \Delta$) and the inequality $\Delta << R$ held. In the present work, all results have been obtained for $\Delta = 4\delta$, where δ has been determined according to the analytical estimate

$$\delta = H\mathrm{Ra_i}^{-1/5}\,. \tag{22}$$

Calculations of meshes with transversal scales $\Delta = 2\delta$ and $\Delta = 3\delta$ give an error in the distribution of the heat flux to the boundary of less than 5%. Besides the cross-section of the calculated region, independent parameters of the problem are also the modified Rayleigh number $\mathrm{Ra_i}$, the Prandtl number Pr, and the aspect ratio R/H. The influence of the latter two parameters has not been investigated in this work and in all numerical experiments they were assumed equal to unity (Pr = 1, $R/H = 1$). Thus, in view of Eq. (22) the only independent parameter of the problem is the modified Rayleigh number $\mathrm{Ra_i}$.

The numerical solution of the equation of motion for the BL (15)–(17) was performed with the use of the implicit difference scheme requiring a choice of the initial temperature profile in the main volume $\widetilde{T}_{\mathrm{b}}$:

$$\widetilde{u}_j^{\,s}\frac{\widetilde{u}_j^{\,n}-\widetilde{u}_j^{\,n-1}}{\Delta\widetilde{z}}+\widetilde{v}_j^{\,s}\frac{\widetilde{u}_{j+1}^{\,n-1}-\widetilde{u}_{j-1}^{\,n-1}}{2\Delta\widetilde{y}}-\frac{\Delta}{R}\frac{\widetilde{u}_{j+1}^{\,n-1}-2\widetilde{u}_j^{\,n-1}+\widetilde{u}_{j-1}^{\,n-1}}{(\Delta\widetilde{y})^{2}}=\widetilde{T}_j^{\,s}-\widetilde{T}_{\mathrm{b}}^{\,s}\,, \tag{23}$$

$$\widetilde{u}_j^{\,s}\frac{\widetilde{T}_j^{\,n}-\widetilde{T}_j^{\,n-1}}{\Delta\widetilde{z}}+\widetilde{v}_j^{\,s}\frac{\widetilde{T}_{j+1}^{\,n-1}-\widetilde{T}_{j-1}^{\,n-1}}{2\Delta\widetilde{y}}-\frac{\Delta}{R}\mathrm{Pr}^{-1}\frac{\widetilde{T}_{j+1}^{\,n-1}-2\widetilde{T}_j^{\,n-1}+\widetilde{T}_{j-1}^{\,n-1}}{(\Delta\widetilde{y})^{2}}=0\,, \tag{24}$$

$$\widetilde{v}_j^{\,n-1}=\widetilde{v}_{j-1}^{\,n-1}-\frac{\Delta\widetilde{y}}{\Delta\widetilde{z}}\left(\widetilde{u}_j^{\,n}-\widetilde{u}_j^{\,n-1}\right). \tag{25}$$

Here the subscript j corresponds to the transverse coordinate $\tilde{y}$ and the superscripts n and s — to the longitudinal coordinate $\tilde{z}$; $\Delta\tilde{z}$ and $\Delta\tilde{y}$ are mesh widths on the longitudinal and transverse coordinates respectively. Since Eqs. (23) and (24) are nonlinear, for their linearization an intermediate layer s on the $\tilde{z}$-coordinate was introduced analogously to [10]. At the initial instant of time $s = n$. Then, using the iteration process, we solved system (23)–(25) by the sweep method, and in so doing, a new s-layer was calculated each time until the square root from the sum of squared residuals became smaller than the given threshold number

$$\sqrt{\sum_j \left(\left(\tilde{u}_j^{n-1} - \tilde{u}_j^s\right)^2 + \left(\tilde{v}_j^{n-1} - \tilde{v}_j^s\right)^2 + \left(\tilde{T}_j^{n-1} - \tilde{T}_j^s\right)^2\right)} < \varepsilon . \tag{26}$$

Only after that could we consider that the $n-1$th layer had been counted up. The whole process was continued until the "bottom," which corresponds to the value of $n = 1$ or $\tilde{z} = 0$, was reached.

After the BL was counted up, the velocity in the main volume was calculated by integrating Eq. (19) by the trapezium method. Likewise, from Eq. (20) a new value of the temperature on the "bottom" was found. Then the temperature in the main volume and the error $\sqrt{\sum_n \left(\tilde{T}_{\text{b}}^{n,i+1} - \tilde{T}_{\text{b}}^{n,i}\right)^2}$, where i is the iteration number, were determined from Eq. (18). The iteration process was continued until the condition

$$\sqrt{\sum_n \left(\tilde{T}_{\text{b}}^{n,i+1} - \tilde{T}_{\text{b}}^{n,i}\right)^2} < \varepsilon \tag{27}$$

was fulfilled.

The solutions of system (15)–(20) are five files $\tilde{u}$, $\tilde{v}$, $\tilde{T}$, $\tilde{U}$, $\tilde{T}_{\text{b}}$. The dimensionless density of the heat flux to the boundary was calculated by the formula

$$\tilde{q}\,(\tilde{z}) = \frac{\tilde{T}\,(\tilde{z}, \Delta\tilde{y})}{\Delta\tilde{y}} . \tag{28}$$

The average heat flux to the boundary is defined by the integral

$$\overline{Q} = \int_0^1 \tilde{q}\,(\tilde{z})\, d\tilde{z} . \tag{29}$$

From Eq. (29) and the dedimensionalization conditions for the mean Nusselt number we have

$$\text{Nu} = \frac{H}{\Delta} \frac{\tilde{q}}{\tilde{T}_{\max}} , \tag{30}$$

where $\tilde{T}_{\max}$ is the maximum temperature in the volume. The calculation was performed in the range of modified Rayleigh numbers $10^6 \le \text{Ra}_{\text{i}} \le 10^{12}$. In this process, the value of the average heat flux was calculated each time by formula (30). Likewise, dedimensionalization and construction of finite-difference equations for the hemispherical geometry was performed. It should be noted that the results have been obtained for $\theta_0 = \arccos\,(1 - \Delta/R)$.

Results and Discussion. The system of equations with boundary conditions (1)–(13) was solved numerically in the range of modified Rayleigh numbers $10^6 \le \text{Ra}_{\text{i}} \le 10^{12}$. As mentioned above, the dependence of the heat transfer characteristics on the aspect ratio and the Prandtl number was not investigated. In all calculations, it was assumed that the Prandtl number was equal to unity, and the radius of the volume was equal to its height. The dimensionless characteristics of free convection in a cylinder and a hemisphere are given in Figs. 3–7. The calculation curves confirm the nonmonotonic temperature profile in the boundary layer in the lower part of the volume [6, 9], which promotes

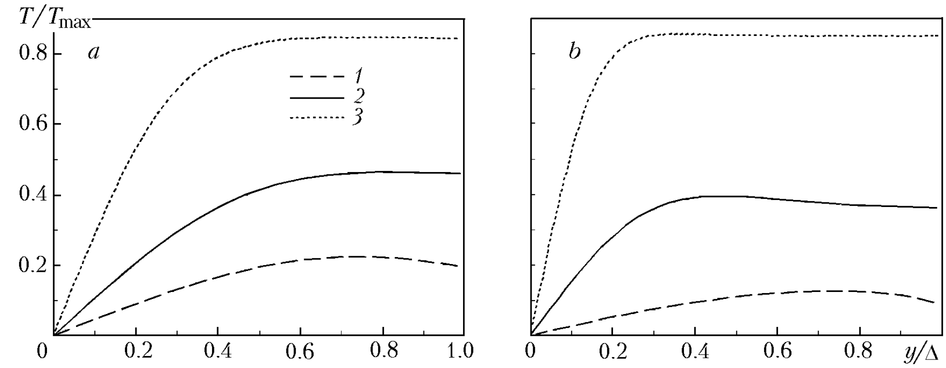

Fig. 3. Temperature in the boundary layer [a) cylinder, b) hemisphere, $Ra_i = 10^{10}$]: 1) $z/H = 0.1$; 2) 0.5; 3) 0.9.

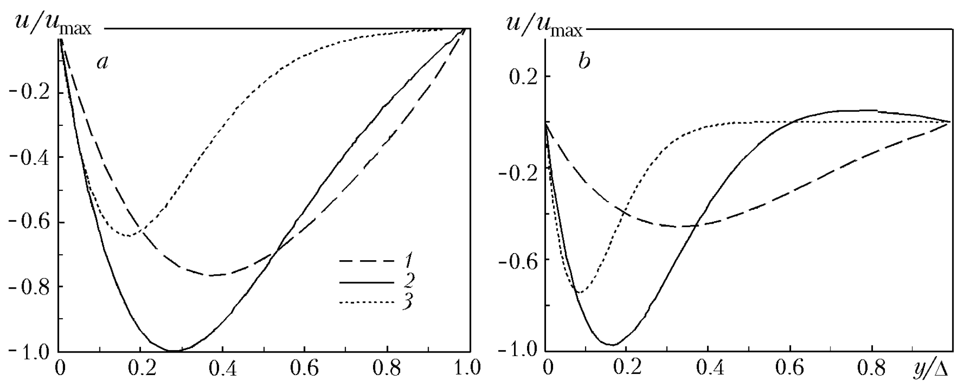

Fig. 4. Longitudinal velocity component in the boundary layer. Notation same as in Fig. 3.

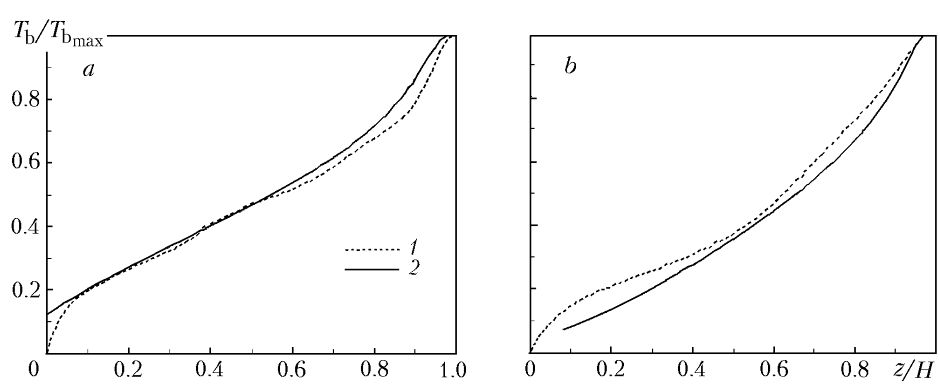

Fig. 5. Temperature in the main volume [a) cylinder, b) hemisphere, $Ra_i = 10^{10}$]: 1) FLUENT; 2) simplified calculation.

the deceleration of the fluid flow, (Fig. 3). From Fig. 4 it is seen that at the outer boundary of the BL ($y = 1$) the derivative of the longitudinal velocity does not vanish, which points to the existence of a return flow which is neglected in the present work. However, comparison with the result of the direct numerical simulation shows that such neglect leads to an error in the distribution of the heat flux to the boundary of no more than 1%. The temperature profile in the main volume (Fig. 5) as well as the distribution of the heat transfer to the lateral boundary agree with the results of the direct numerical simulation performed with the use of the FLUENT program package. The heat flux density reaches its maximum near the upper horizontal boundary (Fig. 6), which also agrees with the results of the ex-

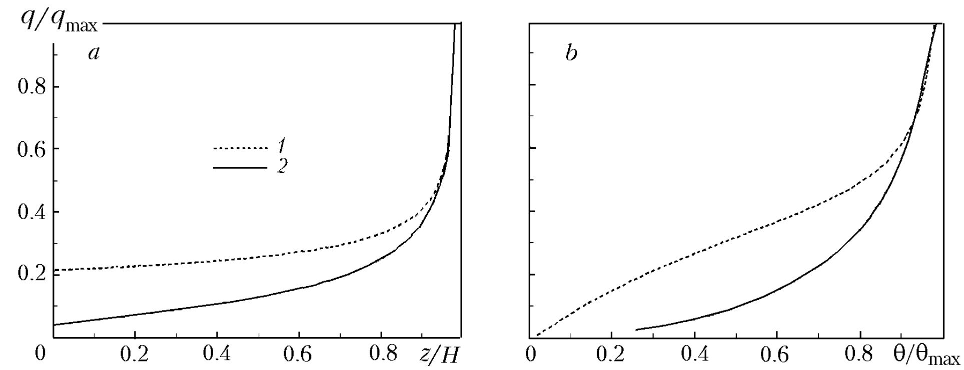

Fig. 6. Density of the heat flux to the boundary [a) cylinder, b) hemisphere, $Ra_i = 10^{10}$]: 1) energy-releasing fluid; 2) constant temperature in the volume.

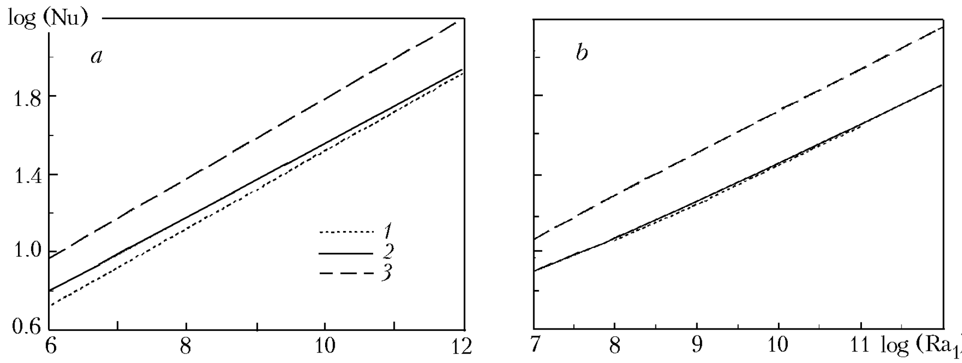

Fig. 7. Integral heat flux [a) cylinder, b) hemisphere]: 1) direct numerical simulation (FLUENT); 2) simplified calculation; 3) constant temperature in the volume.

periments and numerical calculations [6, 7]. Interpolation of the numerical results for the mean Nusselt number through the lateral (in the case of a hemisphere, lower) boundary led to the following correlations:

cylinder

$$\mathrm{Nu_{sd}} = 0.45\mathrm{Ra_i}^{0.19}\,, \quad 10^6 \le \mathrm{Ra_i} \le 10^{12}\,; \tag{31}$$

hemisphere

$$\mathrm{Nu_{dn}} = 0.44\mathrm{Ra_i}^{0.18}\,, \quad 10^7 \le \mathrm{Ra_i} \le 10^{12}\,. \tag{32}$$

The results of the calculation qualitatively agree with the results of the experiments [4, 6]. The existing discrepancy in the mean Nusselt number (see Tables 1 and 2) is explained by the difference in the Prandtl number, the energy release power, and the aspect ratio ($R/H = 1/3$ in [6]). Comparison with the results of the direct numerical simulation performed with the use of the FLUENT program package has not revealed significant discrepancies, especially at high Rayleigh numbers. The existing difference is explained by the neglect of the heat abstraction into the bottom in the proposed model (see (12), (13)).

In a number of engineering applications [12], in calculating convective flows in closed cavities, the temperature stratification in the main volume is neglected. Correlation (31) differs from the formula for the convection of a non-heat-releasing fluid near a vertical semi-infinite plane with a constant temperature at a distance from solid boundaries [13] (Polhausen problem)

TABLE 1. Mean Nusselt Number on the Lateral Boundary (calculation results, cylinder)

Source (experiment, calculation, model)	Correlation		
	Nu_{sd}	Ra_i	Pr
Simplified calculation	$0.45Ra_i^{0.19}$	$10^6 \le 10^{12}$	1
Polhausen problem	$0.55Ra_i^{0.21}$	$10^6 \le 10^{12}$	1
Holzberger's calculation	$0.66Ra_i^{0.2}$	$3{\cdot}10^{10} \le 10^{13}$	7
Direct numerical simulation (FLUENT)	$0.33Ra_i^{0.2}$	$10^6 \le 10^{12}$	1

TABLE 2. Mean Nusselt Number on the Lower Boundary (calculation results, hemisphere)

Source (experiment, calculation, model)	Correlation		
	Nu_{dn}	Rai	Pr
Simplified calculation	$0.45Ra_i^{0.18}$	$10^7 \le 10^{12}$	1
Constant temperature in the volume	$0.46Ra_i^{0.2}$	$10^7 \le 10^{12}$	1
Mayinger's experiment	$0.54Ra_i^{0.18}$	$10^7 \le 5{\cdot}10^{10}$	7
Direct numerical simulation (FLUENT)	$0.39Ra_i^{0.19}$	$10^8 \le 10^{11}$	1

$$Nu_{sd} = 0.54Ra^{1/4} \tag{33}$$

or for the modified Rayleigh number

$$Nu_{sd} = 0.55Ra_i^{0.21} \; . \tag{34}$$

The graphs of the heat flux distribution along the lateral surface and the mean Nusselt number presented in Figs. 6 and 7 point to a significant difference between the convection of a heat-releasing fluid and a fluid without internal heat sources with a constant temperature at a distance from solid boundaries. This is particularly true for the lower part of the volume where the influence of the temperature stratification in the main volume on the structure of the boundary layer increases. In this region, the values of the heat flux densities in the case of an energy-releasing fluid and a fluid without internal heat sources with a constant temperature in the main volume differ by a factor of 7.

As follows from Tables 1 and 2, an important factor influencing the heat transfer distribution is the volume geometry. For the hemispherical geometry in [9] on the basis of an analysis of the dimensionalities and the mass, momentum, and energy balance conditions, simple analytical estimates have been obtained for the heat transfer characteristics of a fluid with internal heat sources in the lower part of the volume. Analogous reasonings for the case of the cylindrical geometry have also made it possible to obtain qualitative estimates for the heat transfer characteristics:

cylinder

$$\bar{u}\,(z) \propto \text{const}\,, \quad q\,(z) \propto c + dz\,, \quad T_b\,(z) \propto a + bz\,; \tag{35}$$

hemisphere

$$\bar{u}\,(\theta) \propto \theta^{9/5}\,, \quad q\,(\theta) \propto \theta^2\,, \quad T_b\,(z) \propto z^{4/5}\,, \tag{36}$$

where $\bar{u}$ is the mean value of the longitudinal velocity modulus in the boundary layer; a, b, c, d are constants. From a comparison of (35) and (36) it follows that the heat flux distribution along the volume boundary in the case of a hemispherical and a cylindrical volumes is different. This is also confirmed by the results of the numerical calculation (see Fig. 6).

Conclusions. A physical model has been constructed and a numerical algorithm for solving the problem on free convective transfer of the heat of an energy-releasing fluid in a closed volume has been developed. We have solved numerically the problem of laminar flow in a cylindrical and hemispherical volumes with an isothermal condition on the lateral (in the case of a hemisphere, lower) boundary in the range of modified Rayleigh numbers $10^6 \le \mathrm{Ra_i} \le 10^{12}$. According to the results of the calculation the dependence of the average dimensionless heat flux (Nusselt number) to the lateral (in the case of a hemisphere, lower) boundary on the modified Rayleigh number has been obtained. The obtained velocity and temperature distributions in the boundary layer on the lateral boundary agree in their structure with the results of experiments and numerical calculations. The influence of the temperature stratification in the main volume on the heat transfer characteristics has been investigated. It turned out that neglect of the stratification in calculating the integral density distribution of the heat flux to the boundary can lead to an overestimation by a factor of more than 2, and in the case of the local heat flux density distribution, to an overestimation by a factor of 7.

The authors wish to thank Prof. V. M. Goloviznin and Candidate of Science E. F. Nogotov (deceased) for consultations on numerical methods.

This work was supported by the Russian Foundation for Basic Research (project 05-08-17964).

NOTATION

A_u, scale factor with velocity dimensionality, m/sec; A_T, scale factor with temperature dimensionality, K; c_p, specific heat capacity, J/(kg·K); g, free fall acceleration, m/sec^2; H, height of the volume, m; Nu, Nusselt number; Pr $= \nu/\chi$, Prandtl number; Q, density of heat sources, W/m^3; q, heat flux density, W/m^2; R, radius of curvature of the lower cooled boundary (for a hemispherical volume), m; $\mathrm{Ra_i} = \dfrac{g\beta QH^5}{\nu\chi\lambda}$, modified Rayleigh number; $S_{\rm up}$, $S_{\rm sd}$, and $S_{\rm dn}$, upper, side, and lower parts of the boundary, respectively; $T \equiv T(z, y)$ (in the case of a hemisphere, $T \equiv T(\theta, y)$), temperature difference of the fluid at a current point (z, y) (for a hemisphere (θ, y)) and the cooled wall, K; T_0, temperature of the cooled part of the boundary, K; $T_{\rm b}$, temperature difference of the fluid outside the boundary layers and the cooled boundary, K; $T_{\rm max}$, maximum temperature difference between the fluid and the cooled boundary, K; $U(z)$, vertical velocity component in the main volume, m/sec; u, longitudinal velocity in the BL, m/sec; v, transverse velocity in the BL, m/sec; V_+ and V_-, regions of the volume higher and lower than the maximum point of the temperature, respectively; y, transverse coordinate counted off from the lateral (in the case of a hemisphere, lower) boundary, m; z, vertical coordinate, m; β, thermal expansion coefficient, K^{-1}; Δ, cross-section of the calculated region for the BL, m; δ, BL thickness on the cooled boundary, m; ε, calculated residual threshold; λ, heat conductivity coefficient, W/(m·K); ν, kinematic viscosity, m^2/sec; ρ, density, kg/m^3; θ, polar angle (for a hemispherical volume), rad; $\chi = \lambda/(\rho c_p)$, thermal diffusivity, m^2/sec. Subscripts: b, quantities pertaining to the main volume; i, internal heat source; j, n, s, integer mesh indices corresponding to coordinates $y(j)$ and $z(n, s)$; dn, sd, up, lower, side, and upper parts of the boundary, respectively.

REFERENCES

1. A. S. Ignat'ev, A. E. Kiselev, V. N. Semenov, V. F. Strizhov, A. S. Filippov, *GEFEST: Numerical Simulation of the Processes in the Lower Part of a WCWMP Reactor in a Bad Accident* [in Russian], Preprint No. IBRAE-2003-13, Moscow (2003).
2. A. E. Kiselev, V. N. Semenov, V. F. Strizhov, A. S. Filippov, and A. S. Fokin, *GEFEST: Models of Heat Exchange with Vapor and Transport of Materials in the LCC of the WCWMP Reactor in a Bad Accident* [in Russian], Preprint No. IBRAE-2003-14, Moscow (2003).

3. M. Jahn, *Holografische Untersuchung der freien Konvektion in volumetrisch beheiten Fluiden*, Doktor-Ingenieur Dissertation, Hannover (1975.)
4. F. Mayinger, M. Jahn, H. Reineke, und U. Steinberner, Untersuchung thermohydrraulischer Vorgänge sowie warmeaustausch in der kernschmelye — optische geschwindigkeitsmessung bei freier Konvektion mit inneren Wärmequellen, *BMFT RS 48/1 Abschlußbericht*, Teil I, Juli 1975.
5. D. Alvarez, P. Malterre, and J. Seiler, Natural convection in volume heated liquid pools — the BAFOND experiments: proposal for new correlations, *Science and Technology of Fast Reactor Safety*, BNES, London (1986), pp. 331–336.
6. M. Holzbecher and A. Steiff, Laminar and turbulent free convection in vertical cylinders with internal heat generation, *Int. J. Heat Mass Transfer*, **38**, No. 15, 2893–2903 (1995).
7. L. A. Bolshov, R. V. Arutyunyan, V. V. Chudanov, et al., Numerical study of natural convection of a heat-generating fluid in nuclear reactor safety problem, *Nuclear Sci. J.*, **32**, No. 2, 134–139 (1995).
8. L. D. Landau and E. M. Lifshits, *Hydrodynamics* [in Russian], Nauka, Moscow (1986).
9. L. A. Bol'shov, P. S. Kondratenko, and V. F. Strizhov, Free convection of a heat-releasing fluid, *Usp. Fiz. Nauk*, **171**, No. 10, 1051–1070 (2001).
10. E. F. Nogotov and A. K. Sinitsyn, On the Numerical investigation of nonstationary convection problem, *Inzh.-Fiz. Zh.*, **31**, No. 6, 1113–1119 (1976).
11. S. K. Godunov and V. S. Ryaben'kii, *Difference Schemes* [in Russian], Nauka, Moscow (1973).
12. G. N. Poletaev, Heat transfer from curvilinear boundaries of heat-generating pools, *Proc. of the NURETH-11* (2005).
13. B. Gebhart, Y. Jaluria, R. L. Mahajan, and B. Sammaki, *Buoyancy-Induced Flows and Transport* [Russian translation], Mir, Moscow (1991).